Journal of The Electrochemical Society, **158** (11) D647-D650 (2011)
0013-4651/2011/158(11)/D647/4/$28.00 © The Electrochemical Society

Electrodeposition from a Liquid Cationic Cuprous Organic Complex for Seed Layer Deposition

Stijn Schaltin,[a,*] Neil R. Brooks,[b] Linda Stappers,[a,*] Lucia D'Urzo,[a] Harald Plank,[c] Gerald Kothleitner,[c] Christian Gspan,[c] Koen Binnemans,[b,] and Jan Fransaer[a,**,z]**

[a]*Department of Metallurgy and Materials Engineering, and* [b]*Department of Chemistry, Katholieke Universiteit Leuven, B-3001 Leuven, Belgium*
[c]*Graz University of Technology, Institute for Electron Microscopy and Fine Structure Research, 8010 Graz, Austria*

Continuous layers of 20 nm of copper have been deposited on a tantalum substrate from the liquid cationic cuprous organic complex $[Cu(MeCN)_2][Tf_2N]$. This type of ionic liquid, with a high concentration of copper(I) ions permits to achieve high nucleation densities. Furthermore, extremely high overpotentials (up to 5.0 V) can be applied without decomposition of the ionic liquid. The deposition of copper has been investigated by cyclic voltammetry (CV), atomic force microscopy (AFM), scanning electron microscopy (SEM) and transmission electron microscopy (TEM). The resulting copper deposits can be useful as seed layers for aqueous copper filling.
 [DOI: 10.1149/2.035111jes]

Manuscript submitted June 28, 2011; revised manuscript received August 3, 2011. Published October 5, 2011.

Due to their intrinsic ionic conductivity and wide electrochemical window, ionic liquids are interesting non-aqueous electrolytes for the electrodeposition of reactive metals which cannot be deposited from aqueous solutions.[1–5] At first sight, there seems to be no advantages associated with the electrodeposition from ionic liquids of metals which can also be deposited from water e.g. zinc, copper, silver or gold. However, in ionic liquids the deposition of alloys of these metals with compositions not obtainable from aqueous solutions is possible, and these solvents also allow the use of electrodes made of materials that are passivated in the presence of water, such as titanium, niobium or tantalum. A useful application is the deposition of a thin copper metal layer on a tantalum electrode. The possibility of direct deposition of copper on a tantalum barrier is of great importance for the microelectronics industry. In state-of-the-art wafer technology, a barrier layer of Ta/TaN prevents the diffusion of copper into silicon.[6–8] Presently, the copper layer is fabricated via a two-step process. First, a copper seed layer is grown by Physical Vapor Deposition (PVD) and this layer protects the underlying tantalum against oxidation. On top of this seed layer, copper is deposited electrochemically from an aqueous copper(II) sulfate solution until the desired thickness is reached. For through-silicon-vias (TSV), the fabrication of the copper seed layers through vapor techniques is troublesome because of the high aspect ratio, resulting in an uneven distribution of the vapor deposited copper. This leads to further difficulties in the consecutive electrodeposition from aqueous solution.

The electrodeposition and nucleation of copper from aqueous solutions on the naturally oxidized surface of tantalum is described by Emery et al.,[9] Radisic et al.[10] and Zheng et al.[11] The nucleation of copper on tantalum, free of an intervening oxide film, is presented by Wang et al.[12] In their study, this oxide layer is removed by galvanic displacement. To achieve a closed film an electroless step was needed and the presence of the interfacial suboxide TaO could not be excluded. Starosvetsky et al. presented an electrochemical procedure to deposit copper on tantalum without a seed layer.[13] An activation step was used to reduce *in situ* the oxide layer to tantalum metal. Although qualitative copper layers were deposited, visual proof of the absence of an oxide layer between the tantalum barrier and the deposited copper was not given. Kim described the electroplating of copper on tantalum, from which the oxide skin is dissolved anodically in a saturated KOH solution.[14] Although the removal of oxide was not complete due to the presence of interfacial TaO, the wetting of copper on tantalum was significantly improved. A disadvantage of this method is the partial loss of the barrier material in the dissolution step.

In this study we present an electrochemical alternative for vapor deposition techniques to achieve a thin copper seed layer, since electrodeposition is not a line-of-sight process like PVD. If this layer is grown in a through-silicon-via, the TSV can later be filled electrochemically with copper from classic aqueous copper plating baths,[15–18] because as yet, the required superfilling process has not been developed for ionic liquids. We describe how copper can be electrodeposited on tantalum from the liquid metal salt $[Cu(MeCN)_2][Tf_2N]$. Liquid metal salts are ionic liquids in which a metal ion is incorporated into the structure of the ionic liquid, preferably in the cation. A detailed chemical and electrochemical characterization of $[Cu(MeCN)_2][Tf_2N]$ has been reported elsewhere.[19,20] Other examples of cationic liquid metal salts can be found in literature.[21–24]

Experimental

The electrolyte $[Cu(MeCN)_2][Tf_2N]$ was prepared starting from the copper(I) complex tetrakis(acetonitrile) copper(I) bis(trifluoromethylsulfonyl)imide (bistriflimide), $[Cu(MeCN)_4][Tf_2N]$ (figure 1).

The cation of $[Cu(MeCN)_4][Tf_2N]$ consists of four acetonitrile molecules coordinating to the copper(I) ion in a tetrahedral arrangement. The charge balance is provided by the $[Tf_2N]^-$ counter anion. This compound was prepared by reacting copper(II) oxide with bis(trifluoromethylsulfonyl)imidic acid in water to yield copper(II) bistriflimide. Copper metal was then added to a solution of the copper(II) salt in acetonitrile. Because copper(I) is the stable copper species in acetonitrile solutions,[25–27] a comproportionation reaction between copper metal and the copper(II) ions yielded $[Cu(MeCN)_4][Tf_2N]$. The overal reaction scheme is:

$$CuO + 2\ H[Tf_2N] \rightarrow Cu(Tf_2N)_2 + H_2O \qquad [1]$$

$$Cu(Tf_2N)_2 + Cu + 8\ CH_3CN \rightarrow 2\ [Cu(CH_3CN)_4][Tf_2N] \qquad [2]$$

At room temperature, $[Cu(MeCN)_4][Tf_2N]$ is a white crystalline solid that melts at 66°C into a colorless liquid. Two acetonitrile molecules were driven off by equilibrating the compound at 90°C for 24 h to give $[Cu(MeCN)_2][Tf_2N]$. This temperature was chosen because it is the standard temperature at which electrochemical experiments have been performed. So the composition of the electrolyte used for electrodeposition of the copper layers is $[Cu(MeCN)_2][Tf_2N]$.

* Electrochemical Society Student Member.
** Electrochemical Society Active Member.
z E-mail: Jan.Fransaer@mtm.kuleuven.be

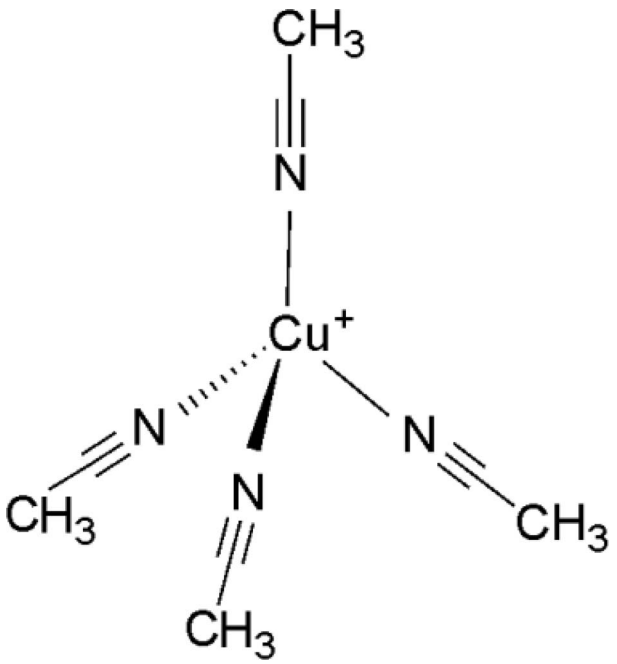

Figure 1. Structural formula of the cation of the copper-containing ionic liquid $[Cu(MeCN)_4][Tf_2N]$.

The electrochemical experiments were performed in an argon-filled glove box (with O_2 and H_2O concentrations below 1 ppm) because the tested low-melting salts are sensitive to moisture and oxygen and undergo oxidation of copper(I). Silicon wafers have been used as the substrates for electrodeposition. The different layers of this wafer were: Si - 100 nm SiO_2 - 10 nm TaN - 40 nm Ta - 150 nm Cu. Before use, these substrates, with an active area of 7 mm by 10 mm, were degreased in alkaline cleaner (type P3-RST, Henkel) at 70°C, rinsed in demineralized water and ethanol, and dried. The copper layer of the wafers was electrochemically dissolved *in situ* just before the deposition experiments. After the deposition of the copper layer, they were rinsed with acetone and ethanol, and finally dried. The copper solution was contained in a copper crucible (5 ml), which also served as counter-electrode, and it was not stirred during the experiments. The experiments were done using an EG&G Princeton Applied Research potentiostat/galvanostat model 273 controlled by a computer with Corrware software (cyclic voltammetry) or an EG&G Princeton Applied Research potentiostat/galvanostat model 263A. All specified potentials in this paper are relative to a copper pseudo-reference electrode. A polyimide Thermofoil™ heater was used to maintain the temperature at 90°C during the experiments. The morphology of the copper deposits was determined by scanning electron microscopy (SEM) (Philips XL 30 FEG) and atomic force microscopy (AFM) (Digital Instruments Nanoscope III AFM). Thin lamellas for transmission electron microscopy (TEM) investigations have been prepared via a NOVA 200 (FEI) dual beam system combining a focused ion beam (FIB) and a scanning electron microscope (SEM). Lamellas have been prepared in standard lift out geometry and subsequently transferred with a micromanipulator (Omniprobe) to TEM grids (Omniprobe). To prevent lamella bending, window milling technique was applied during pre-thinning procedure followed by a low energy cleaning step at 5 kV and 70 pA under an angle of 5° on both sides to reduce amorphized surface layers. All subsequent TEM investigations were performed at 200 kV on a Tecnai T20 FEG/STEM, equipped with a Gatan Quantum EELS spectrometer. For imaging, bright field phase contrast techniques have been applied, whereas for the chemical analysis, the system was set up in scanning TEM mode, employing a beam diameter of approximately 0.5 nm, a beam convergence of about 10 mrad and a collection angle of 15 mrad.

Results and Discussion

The tantalum layer of the silicon wafer was protected against oxidation by a copper seed layer. Before electrodeposition, this seed layer was anodically dissolved at +0.5 V to expose the underlying tantalum to the electrolyte. The resulting current-time plot is shown in figure 2a, which reveals that the current quickly peaks high and eventually drops to zero when all the copper is dissolved. Nonetheless, the anodic polarization was maintained for 400 s in order to dissolve all copper. The cyclic voltammogram, recorded after 400 s of anodic polarization, is shown in figure 2b.

The overall appearance of this cyclic voltammogram is typical for an electrode reaction involving the electrodeposition and stripping of metal. The voltammogram indicates that the nucleation of copper onto tantalum requires an overpotential of 0.1 V. This nucleation overpotential causes the appearance of a nucleation loop: the backward scan of the voltammogram crosses the forwards scan at 0 V.

Deposits were made at overpotentials η in the range from −3.0 V and −5.0 V. In conventional ionic liquids e.g. imidazolium or pyrrolidinium salts, such cathodic overpotentials cannot be applied without the decomposition of the ionic liquid. Also the $[Cu(MeCN)_2][Tf_2N]$ complex is cathodically decomposed, but in this case the decomposition is the desired reduction of Cu(I) into metallic copper

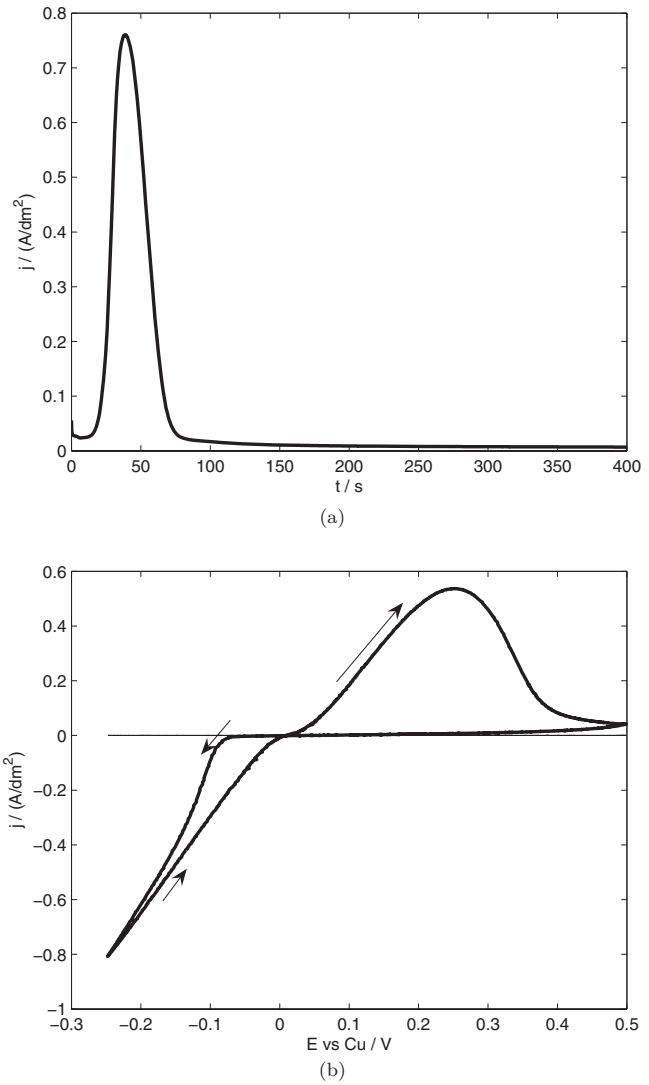

Figure 2. (a) Seed layer stripping at +0.5 V. (b) Cyclic voltammograms of the ionic liquid $[Cu(MeCN)_2][Tf_2N]$ on a tantalum working electrode at 90°C. The scan rate was 50 mV s^{-1}.

without the reduction of acetonitrile or the bistriflimide anion.[20] The liberated acetonitrile molecules become bound to the Cu(I) in $[Cu(MeCN)_2][Tf_2N]$ in the bulk electrolyte, temporarily forming $[Cu(MeCN)_4][Tf_2N]$ or diffuse towards the anode where they assist the anodic dissolution of copper. The net reaction in the electrochemical cell is therefore just the dissolution and deposition of copper, whereas in *regular* ionic liquids the solution would get poisoned by decomposition products of the cation. High applied overpotentials give rise to small sized copper grains. This comes from the electrochemical Kelvin equation[28]

$$r_c = \frac{2\gamma V_{mol}}{nF|\eta|} \quad [3]$$

in which γ is the surface energy between deposit and electrolyte (J m^{-2}), V_{mol} the molar volume of the deposited metal (m^3 mol^{-1}), n the ion charge, F the Faraday constant (C mol^{-1}) and r_c is the critical radius for nucleation (m). A nucleus is only stable and able to grow if its size is equal to, or exceeds r_c. If it is smaller than r_c, it is energetically favorable to dissolve again. By using $\gamma = 0.5$ J m^{-2} [28] and $V_{mol} = 7.1 \cdot 10^{-6}$ m^3 mol^{-1}, a critical nucleus consists of a single atom if an overpotential of $\eta \approx 0.5$ V is applied. Because copper was deposited at more negative potentials than -0.5 V, nucleation can proceed without the need to form clusters of atoms. As a result, nucleation solely depends on the available nucleation sites. The high intrinsic concentration of Cu(I) ions in $[Cu(MeCN)_2][Tf_2N]$ (3.1 mol dm^{-3} [20]) causes that more nucleation sites can start growing simultaneously: growing nuclei will deplete their surroundings of Cu(I) ions which inhibits further nucleation and growth of nucleation sites located in the diffusion layer of the original nucleus. Due to the higher concentration, more time will pass before the concentration drops below levels where no further nucleation occurs and during this time interval more nucleation sites can be activated.

The deposit made at -3.0 V shown in figure 3a has a grainy morphology with varying grain sizes and open grain boundaries. This was also confirmed by TEM analyses of deposit cross-sections with varying layer thickness between 13 and 38 nm. For -4.0 V (figure 3b), the deposit reveal a flat appearance, with a varying grain size but fewer pinholes than the deposit made at -3.0 V (figure 3a). TEM revealed a film thickness around 19 nm. The best results were obtained at -5.0 V: figure 3c shows a deposit with flat appearance, very few pinholes and a thickness around 19 nm, found by TEM measurements (figure 4).

A continuous tantalum oxide layer of 3−5 nm was found along the entire Cu-Ta interface. This oxide layer is indicated by the two parallel lines in figure 4 and it forms most probably during the anodic polarization of the substrate. No oxygen was found at the interface of the tantalum substrate and the originally present copper seed before the latter was anodically dissolved. Some pinholes, through which oxygen can diffuse, are present in the deposits but there are too few of them to permit sufficient oxygen transport to obtain the uniform oxide layer on the copper-tantalum interface, as seen in figure 4c. The composition of the oxide layer was Ta_2O_5, as determined by quantitative EELS compositional analysis in combination with multiple scattering simulations (FEFF code) of the O-K edge fine structure. The adhesion of copper to the tantalum substrate was tested by submitting the deposited layers to the Scotch tape test. All samples that were tested could withstand this test, indicating a good adhesion between tantalum and the deposited copper.

It was tried to describe the nucleation behavior by the well-known theory developed by Scharifker and Hills.[29] According to this theory, the nucleation behavior can be studied by fitting the experimentally measured currents to the theoretical curves for progressive and instantaneous nucleation. This method works fine for small overpotentials and low concentrations for which a clear maximum in current develops a few seconds after applying the potential step. In our experiments, this theory could not be applied. Firstly, the concentration of electroactive species is high (3.1 mol dm^{-3}, see reference[20]), which shifts the current maximum to shorter times. Secondly, the applied overpotentials are high. This causes a large charging current for the electrical double layer which interferes in determining the location and value of the current maximum. The nucleation was therefore determined by the topographical investigation via atomic force microscopy (AFM). Topologies were measured at three deposition potentials (-3.0, -4.0 and -5.0 V) and deposition times as short as 15 ms to calculate the nucleation densities and nucleation rates. Unfortunately, AFM scans show that even for such short deposition times separate nuclei start to coalesce so that an accurate determination of the nucleation rate is not possible since the separate nuclei can no longer be distinguished. A lower limit for the nucleation density N was calculated by the empirical formula $N = (\pi d^2)^{-1}$, in which d,

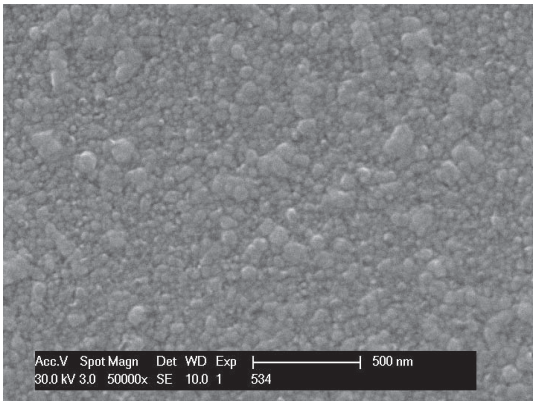

(a)

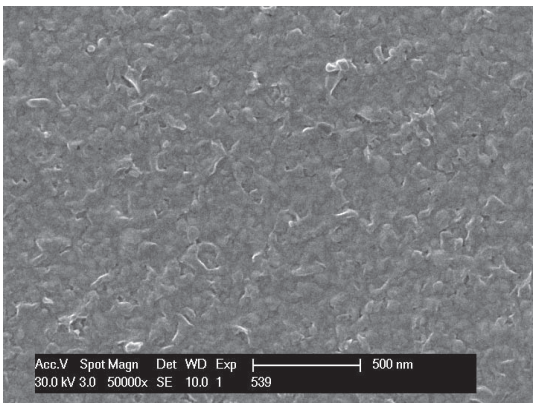

(b)

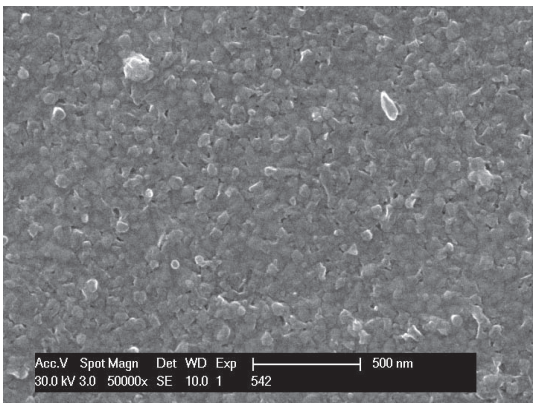

(c)

Figure 3. SEM micrographs of copper deposits from the ionic liquid $[Cu(MeCN)_2][Tf_2N]$ on a tantalum working electrode after seed layer stripping at +0.5 V at 90°C: (a) 0.5 s at −3.0 V, (b) 0.25 s at −4.0 V, (c) 0.25 s at −5.0 V.

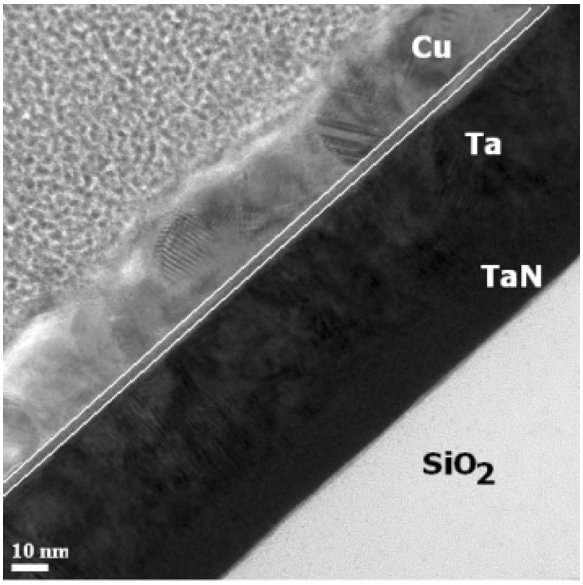

Figure 4. TEM cross-section of a copper deposit from the ionic liquid $[Cu(MeCN)_2][Tf_2N]$ on a tantalum working electrode at 90°C: 0.25 s at −5.0 V. The white lines mark the tantalum oxide layer.

the deposit thickness, was taken from the TEM cross section. This formula is valid in situations in which closed layers have been deposited. Figure 4 shows that this condition is met. The calculated value for N was $N = 8 \cdot 10^{14}$ m^{-2}. This nucleation density is higher than for aqueous deposition on the native tantalum oxide layer where $N \approx 10^{12}$ m^{-2}.[10,11] This high nucleation density, despite the presence of an oxide layer, is due to the large overpotential that can be applied in $[Cu(MeCN)_2][Tf_2N]$ without decomposition products of the ionic liquid poisoning the electrolyte. This makes $[Cu(MeCN)_2][Tf_2N]$ an excellent medium for the electrodeposition of very thin seed layers in non-aqueous environments.

Conclusion

The use of the ionic liquid $[Cu(MeCN)_2][Tf_2N]$ as medium for copper electrodeposition on a tantalum substrate is demonstrated. A nucleation density of $8 \cdot 10^{14}$ m^{-2} is reached at a deposition potential of −5.0 V. The deposits show a flat appearance and very few pinholes for thicknesses around 19 nm. Research towards the origin of the oxide layer (from water, dissolved oxygen, or chemical decomposition of the bistriflimide anion $[Tf_2N]^-$) is ongoing, just as the search for additives that can improve the morphology of the deposited copper. If the oxidation of the tantalum substrate can be avoided, it is most likely that the thickness of the copper deposits can be reduced even further, possibly to about 5 nm. In that case, the layers become thin enough not only as seed layers for TSV, but also for vias and trenches to achieve superfilling.

Acknowledgments

This research was funded by a Ph.D grant of the Institute for the Promotion of Innovation through Science and Technology in Flanders (IWT-Vlaanderen) to S.S. This work is supported in part by the European Commissions Seventh Framework Programme (FP7) under Grant Agreement number 216474 (CopPeR). The authors acknowledge financial support by the K.U.Leuven (projects IDO/05/005 and GOA 08/05), by the FWO-Flanders (research community "Ionic Liquids") and by the IWT-Flanders (SBO-project IWT 80031 "MAPIL"). Support by IoLiTec (Heilbronn, Germany) is also acknowledged.

References

1. F. Endres, A. P. Abbott and D. F. MacFarlane (Eds.), *Electrodeposition from ionic liquids*, Wiley-VCH, Weinheim, (2008).
2. F. Endres and S. Zein El Abedin, *Phys. Chem. Chem. Phys.*, **8**, 2101 (2006).
3. F. Endres, *ChemPhysChem*, **3**, 144 (2002).
4. F. Endres, *Z. Phys. Chem.*, **218**, 255 (2004).
5. A. P. Abbott and K. J. McKenzie, *Phys. Chem. Chem. Phys.*, **8**, 4265 (2006).
6. T. Oku, E. Kawakami, M. Uekubo, K. Takahiro, S. Yamaguchi and M. Murakami, *Appl. Surf. Sci.*, **99**, 265 (1996).
7. M. T. Wang, Y. C. Lin and M. C. Chen, *J. Electrochem. Soc.*, **145**, 2538 (1998).
8. K. Holloway, P. M. Fryer, C. Cabral, J. M. E. Harper, P. J. Bailey and K. H. J. Kellegher, *J. Appl. Phys.*, **71**, 5433 (1992).
9. S. B. Emery, J. L. Hubbley and D. Roy, *J. Electroanal. Chem.*, **568**, 121 (2004).
10. A. Radisic, G. Oskam and P. C. Searson, *J. Electrochem. Soc.*, **151**, C369 (2004).
11. M. Zheng, J. J. Kelly and H. Deligianni, *J. Electrochem. Soc.*, **154**, D400 (2007).
12. Z. Wang, H. Li, H. Shodiev and I. I. Suni, *Electrochem. Solid-State Lett.*, **7**, C67 (2004).
13. D. Starosvetsky, N. Sezin and Y. Ein-Eli, *Electrochim. Acta*, **55**, 1656 (2010).
14. S. Kim, *Electrochem. Solid-State. Lett.*, **13**, D83 (2010).
15. P. C. Andricacos, C. Uzoh, J. O. Dukovic, J. Horkans and H. Deligianni, *IBM J. Res. Develop.*, **42**, 567 (1998).
16. W.-P. Dow, H.-H. Chen, M.-Y. Yen, W.-H. Chen, K.-H. Hsu, P.-Y. Chuang, H. Ishizuka, N. Sakagawa and R. Kimizuka, *J. Electrochem. Soc.*, **155**, D750 (2008).
17. O. Lühn, A. Radisic, P. M. Vereecken, C. Van Hoof, W. Ruythooren and J.-P. Celis, *Electrochem. Solid-State Lett.*, **12**, D39 (2009).
18. O. Lühn, C. Van Hoof, W. Ruythooren and J.-P. Celis, *Electrochim. Acta*, **54**, 2504 (2009).
19. N. R. Brooks, S. Schaltin, K. Van Hecke, L. Van Meervelt, K. Binnemans, and J. Fransaer, *Chem. Eur. J.*, **17**, 5054 (2011).
20. S. Schaltin, N. R. Brooks, K. Binnemans and J. Fransaer, *J. Electrochem. Soc.*, **158**, D21 (2011).
21. J.-F. Huang, H. Luo and S. Dai, *J. Electrochem. Soc.*, **153**, J9 (2006).
22. H. M. A. Abood, A. P. Abbott, A. D. Ballantyne and K. S. Ryder, *Chem. Commun.*, **47**, 3523 (2011).
23. M. Iida, C. Baba, M. Inoue, H. Yoshida, E. Taguchi and H. Furusho, *Chem. Eur. J.*, **14**, 5047 (2008).
24. M. Iida, S. Kawakami, E. Syouno, H. Er and E. Taguchi, *J. Colloid Interface Sci.*, **356**, 630 (2011).
25. S. G. Biallozor, *Electrochim. Acta*, **17**, 1243 (1972).
26. S. G. Biallozor and D. Poletek, *Élektrokhimiya*, **15**, 472 (1979).
27. N. Petrescu, L. Ganovici and M. Britchi, *Rev. Roum. Chim.*, **29**, 407 (1984).
28. E. Budevski, G. Staikov and J. W. Lorenz, in *Electrochemical Phase Transformation and Growth* VCH, Weinheim (1996) p161-162.
29. B. Scharifker and G. Hills, *Electrochim. Acta*, **28**, 879 (1983).